

Pattern recognition in low-resolution instrumental tactile imaging

Stepan A. Nersisyan and Yan I. Rakhmatulin

Abstract—Background. Tactile perception is an essential source of information. However instrumental registration and automated analysis of tactile data is still at an initial point of the development. Recently a Medical Tactile Endosurgical Complex (MTEC) has been introduced into clinical practice as a universal instrument for intrasurgical registration of tactile images. Images registered by MTEC have very limited resolution both in terms of a number of tactile pixels and a number of discretization levels. In this study we investigated whether this resolution is sufficient for reliable pattern recognition.

Methods. Our study used a set of artificial samples which included six sample types. In particular, four of these types directly tested the ability to discriminate patterns with the same embedment projection sizes but different curvatures, or similar curvatures but different projection sizes. Two widely used machine learning methods were evaluated: random forests and k -nearest neighbors. These methods were applied to points representing registered tactile images in a relatively low-dimensional feature space. Additionally an in-silico cloning of images was used to increase classification reliability.

Results. Both classification methods – random forests and k -nearest neighbors – showed good classification reliability with accuracy 68.6% and 72.9% on the validation set, respectively. These values are more than four times higher than an accuracy of six-class “random classifier”. Random forests additionally provided evaluation of importance of features used for classification.

Conclusion. Despite poor resolution of tactile images registered by MTEC a combination of conventional machine learning methods with a specific feature set and specific tricks provides highly reliable results of automated analysis of these images even in case of nontrivial tasks such as sample classification with very similar classes.

Keywords—Classification, k -nearest neighbors, Medical Tactile Endosurgical Complex, random forests, tactile image.

I. INTRODUCTION

TACTILE perception is an essential source of information. However instrumental registration and automated analysis of tactile data is still at an initial point of the development. At the same time, recently a number of specialized medical

The research was supported by the Russian Science Foundation (project 16-11-00058 “The development of methods and algorithms for automated analysis of medical tactile information and classification of tactile images”).

S. A. Nersisyan is with the Faculty of Mechanics and Mathematics, Lomonosov Moscow State University, Leninskie Gory 1, Moscow 119991, Russia (phone: +7 (985) 125-23-00; fax: +7 (495) 939-20-90; e-mail: s.a.nersisyan@gmail.com).

Y. I. Rakhmatulin is with the Faculty of Mechanics and Mathematics, Lomonosov Moscow State University, Leninskie Gory 1, Moscow 119991, Russia (e-mail: nyaq@yandex.ru).

devices for instrumental registration of tactile images have been designed and introduced into clinical practice. Whereas the majority of these devices, such as Breast Mechanical Imager [1], Vaginal Tactile Imager [2], [3] or Prostate Mechanical Imaging System [4], have a narrow (organ-specific) application domain, Medical Tactile Endosurgical Complex (MTEC) [5], [6] is more universal. MTEC has been designed to perform instrumental palpation in minimally-invasive surgery, where conventional (manual) palpation is impossible, providing identification and localization of visually undetectable pathologies. This complex is successfully applied in thoracoscopic surgery (where its utilization decreases the conversion rate [5]) and gastrointestinal surgery [7,8]. In robot-assisted surgery MTEC partially solves the problem of insufficient feedback related to touch [6].

A tactile mechanoreceptor, which is a key component of MTEC, allows tactile inspection of an arbitrary sample with a flat or almost flat surface. But inspection results have very limited resolution both in terms of a number of tactile pixels and a number of discretization levels, and in clinical applications they are used mainly for manual or automated identification of heterogeneities associated with lesion boundaries [6], [9], without subsequent deeper analysis of registered tactile images. In this research we investigated whether this resolution is sufficient for reliable pattern recognition. More specifically, we evaluated the results of classification of instrumentally registered tactile images into six predefined classes using two widely applied machine learning approaches – random forests [10] and k -nearest neighbors [11], [12].

II. MATERIALS AND METHODS

A. A structure of tactile images

MTEC registers tactile images with a tactile mechanoreceptor (Fig. 1). This device has an operating head with either 7 or 19 pressure sensors which geometrically form a non-rectangular grid associated with a hexagonal plane tessellation (Fig. 2). A diameter of these operating heads is 10 mm and 20 mm, respectively. During a press on an examined sample sensors simultaneously perform pressure measurements, a mechanoreceptor combines these values into a frame and sends it to a computer for the processing and analysis. The measurement frequency is 100 Hz, and the number of discretization levels after preprocessing is 256.



Fig. 1. MTEC tactile mechanoreceptor with 7 sensors (a) and 19 sensors (b).

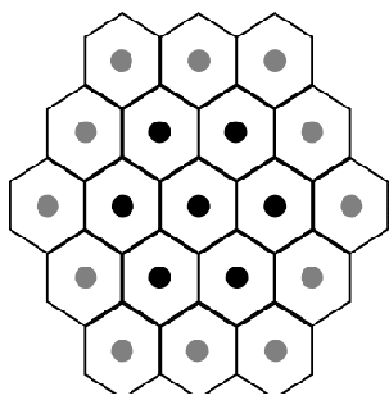


Fig. 2. Location of pressure sensors on an operating head of a MTEC tactile mechanoreceptor. Sensors are shown by circles; for each sensor an associated cell of a hexagonal plane tessellation is depicted. Seven-sensor version of a tactile mechanoreceptor has only sensors colored in black.

Thus, an individual tactile frame consists of 8-bit pressure values associated with 7 or 19 pixels, and a tactile image consists of several hundreds of consecutive tactile frames. In this research we consider the case of 19-pixel frames (i.e., use 19-sensor mechanoreceptor for registration of tactile images).

A press on an examined sample by a tactile mechanoreceptor is performed manually, so differences in pressing parameters are inevitable. Moreover, if a sample is examined twice with a slight shift or slight rotation of an operating head in one examination in comparison with the other one, registered tactile frames (considered as points in a

19-dimensional space or as arrays with 19 elements) can differ essentially. For example, in one examination a small firm embedment in a soft sample can be located against one sensor, so only one pressure value will achieve high levels, but after a small shift this embedment can be detected by two or more adjacent sensors, leading to several high values (Fig. 3). Larger shifts and rotations can lead to more essential changes of registered tactile frames (Fig. 4). Thus, tactile images associated with the same sample can be significantly different, and it is really observed in clinical applications, where an orientation (e.g., an axial rotation) of a mechanoreceptor operating head with respect to a lesion is uncontrolled and random.

B. A structure of a set of tactile images

In order to test whether resolution of MTEC is sufficient for pattern recognition, we manufactured samples of six types. Similarly to [13], [14], the samples were made of a soft silicone (Shore hardness 00-10A) and had a shape of a rectangular block with size 40 mm × 35 mm × 10 mm. The difference between types was in embedments:

- *E-type* samples were homogeneous (i.e., contained no embedment);
- *LF-type* and *LC-type* samples contained a firm embedment which had a form of a spherical cap with base diameter 8 mm and height 2.4 mm, oriented for palpation from the convex side and the flat side, respectively;
- *SF-type* and *SC-type* samples were similar, but have a different size of embedment (base diameter 4.7 mm and height 1.7 mm);

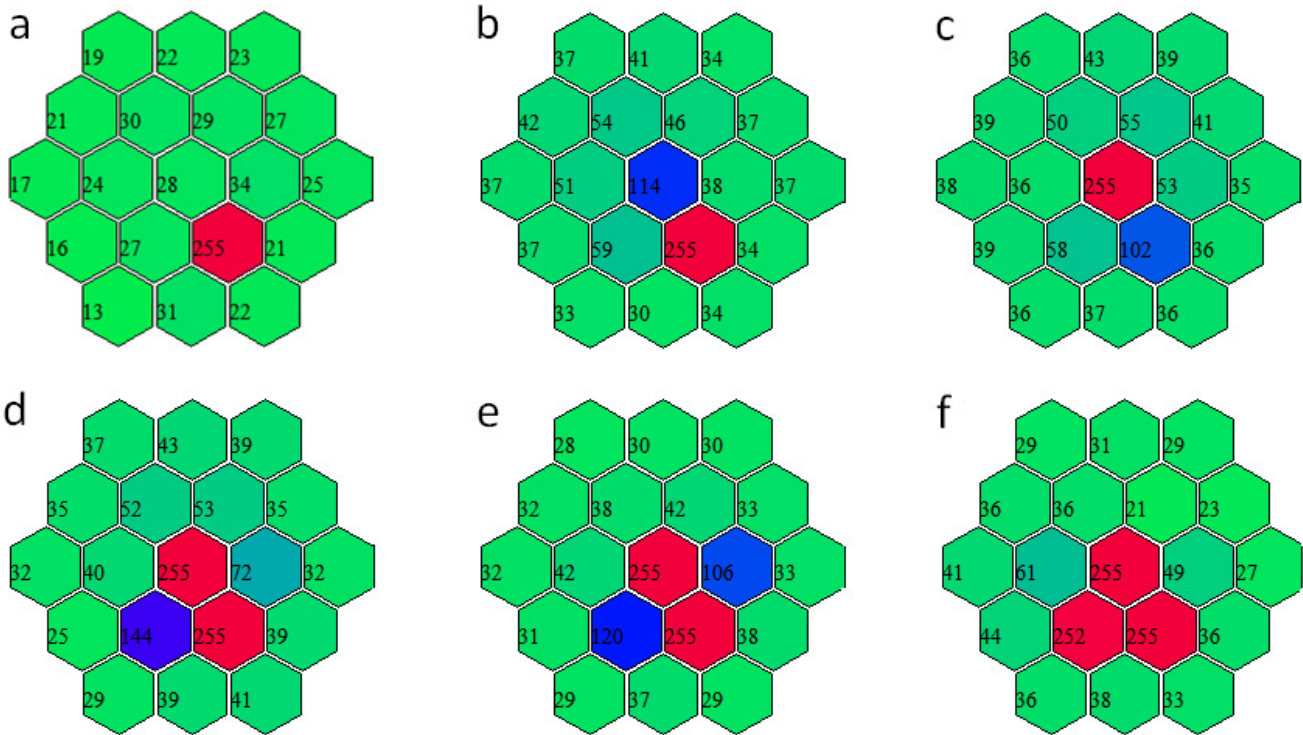


Fig. 3. Tactile frames registered by MTEC mechanoreceptor during presses on a small firm embedding in a soft sample. Registered pressure values are shown in hexagonal cells associated with sensors both by numbers and color-code (in a green-blue-red color scale [6]). Presses slightly differed in a shift and a rotation of a mechanoreceptor operating head.

– *T-type* samples contained a segment of a medical perfusion line (B. Braun Original Perfusion Line, diameter ca 2 mm) as an embedment. This segment had length of at least 20 mm and was oriented horizontally. LF, LC, SF and SC types of samples tested the ability to discriminate patterns with the same embedment projection sizes but different curvatures, or similar curvatures but different projection sizes. T-type samples modeled blood vessels. E-type samples models homogeneous tissue.

Two lots of samples were manufactured independently. The first one was used for construction and tuning of classifiers and the second one was used for an independent validation. The first lot contained at least 6 samples for each type. Multiple examinations of these samples resulted in a training set of tactile images with 100 images per type. The second lot contained at least 4 samples for each type which multiple examinations resulted in a validation set with 40 tactile images per type. An instrumental tactile examination of the samples from the first lot and the second lot was performed with different tactile mechanoreceptors and by different operators, thus pressing parameters for the training and for the validation sets of tactile images were different.

C. Most informative frame and other features

In order to reduce dimension and simultaneously reduce dependence on tactile examination parameters (e.g., pressing speed), in a tactile image we found a frame with maximum intra-frame standard deviation. We called it *the most*

informative frame of the tactile image and used it to form a set of input features for classifiers. More specifically, we replaced each value in the most informative frame by a mean over a series of adjacent frames (thus utilizing a standard smoothing procedure for noise filtration), scaled these values to [0, 1] segment applying formula

$$y_j = \sqrt{\frac{x_j - x_{min}}{x_{max} - x_{min}}}$$

(here x_j is a smoothed unscaled value associated with the j -th sensor, x_{min} and x_{max} are minimum and maximum values of x over all sensors, y_j is a scaled value), and included resulting scaled values y_j ($j = 1, 2, \dots, 19$) into the feature set. Experiments proved that computation of a square root at the final step of scaling leads to a slight increase of classification reliability in comparison with scaling where this step is omitted.

Additionally, for each sensor we computed standard deviation d_j associated with its measurements in the tactile image, performed scaling

$$v_j = \frac{d_j - d_{min}}{D_{sc}}$$

(scaling coefficient D_{sc} was set to 125) and included M largest scaled deviations v_j into the set of input features as well.

Value of M and other parameters used for feature selection (e.g., a size of series of adjacent tactile frames used for smoothing) were selected on the base of cross-validation (see below).

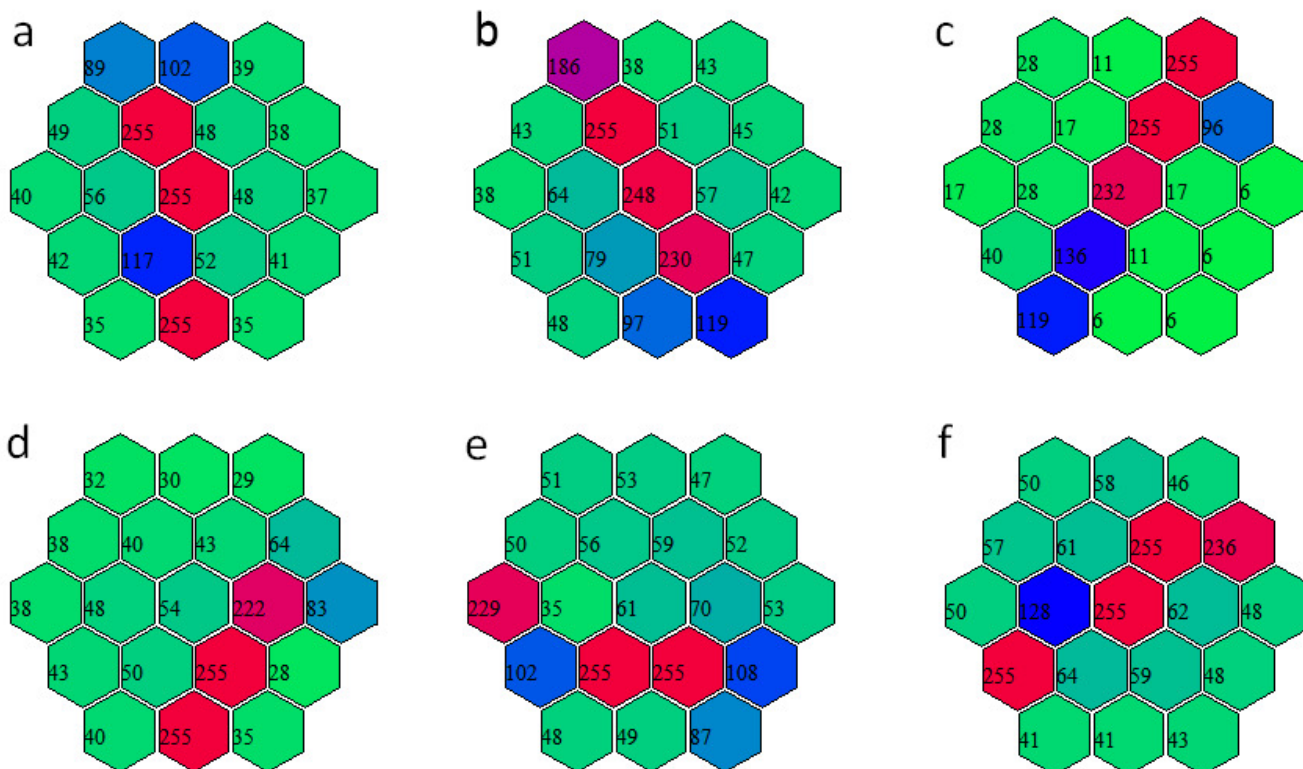


Fig. 4. Tactile frames registered by MTEC mechanoreceptor during presses on a long (vessel-like) embedment in a soft sample. Registered pressure values are shown in hexagonal cells associated with sensors both by numbers and color-code (in a green-blue-red color scale [6]). Presses differed in a shift and a rotation of a mechanoreceptor operating head.

Along with an approach to the selection of the most informative frame based on intra-frame standard deviation we tested several other approaches, including the selection based on maximum-minimum difference, interquartile range, mean absolute deviations. But these alternatives resulted in lower quality of the resulting classification.

D. Classifier tuning

Two classification methods were tested: random forests [10] and k -nearest neighbors [11], [12].

Random forests are an ensemble classification method based on the idea of building a large number of decision trees. In this approach the target class is usually estimated by the voting scheme applied to the outputs of constructed trees. The goal of decision tree classifier is to infer a set of decision rules from the training set and to put these rules into the tree structure. The advantages of random forests classifier include high accuracy, computational performance, resistance to overfitting and ability to give information about importance of features used in the classification process.

K -nearest neighbors classification is based on the following procedure. Each element of a training set is considered as a point in an n -dimensional metric (or generalized metric) space, where n denotes the number of features in the set. The class for unknown data element (which is also associated with a point in the same space) is predicted as the most frequent class in the list of k nearest points of the training set (relative to the space

metric). The advantages of the k -nearest neighbors classification method include robustness to noisy training data and natural handling multi-class cases.

Classifiers tuning was performed using Scikit-Learn Python library [15], in an unweighted version for k -means, and with Gini impurity criterion for random forests.

First, we optimized parameters using multiple 5-fold cross validation based on the training set of tactile images, and then applied the resulting classifier to the validation set of tactile images. Parameter optimization utilized a block-wise greedy scheme.

E. In silico cloning of tactile images

To make classification more reliable, we used the following trick. For each tactile image in the training set we performed in-silico cloning by adding

- results of its rotation by angles multiple to 60° and
- results of symmetric reflections to this set

(the utilized transformations move the sensor-associated grid to itself). Overall, cloning each tactile image generated a set of 12 images, including the one being cloned. Our experiments showed that this trick really provided an increase of classification reliability.

For random forests a similar cloning was applied for an image being classified, and the final class was determined based on 12 classification results using a voting scheme.

III. RESULTS

A. Random forest classifier

Cross-validation showed that for a random forest classifier an optimal series for noise filtration in the most informative frame contains 17 frames, including 10 preceding the most informative one and 6 following it. However, for optimal results only frames from this series which satisfy additional conditions should be utilized for smoothing. These additional conditions can be formulated in terms of sums of unscaled pressure measurement values (i.e., discretized 8-bit values interpreted as an integer from [0, 255] range). Let S be this sum for an arbitrary frame from the series, and S_{inf} be this sum associated with the most informative frame. A frame from the series should be utilized only if

- $S \leq 3000$ (which means that for all or at least almost all sensors saturation level has not been reached), and
- $0.1S_{inf} \leq S \leq 2.0S_{inf}$ (i.e., series frames that are clearly different from the most informative one probably due to a very fast press are excluded).

Thresholds (3000, 0.1, 2.0) were obtained using the same cross-validation.

Then, cross-validation demonstrated that the optimal value of M was 1, and greater values gave visibly lower classification reliability. Thus, 20 features were associated with a tactile image:

- 19 smoothed and scaled pressure values y_j originated from the most informative frame;
- the largest scaled deviation v_j .

A sufficient maximum depth of decision trees was 20 and this parameter was essential. At the same time, a number of decision trees was less essential and could be taken equal to 150. Larger numbers of decision trees did not provide any increase of classification reliability.

For these parameters the results of application of a random

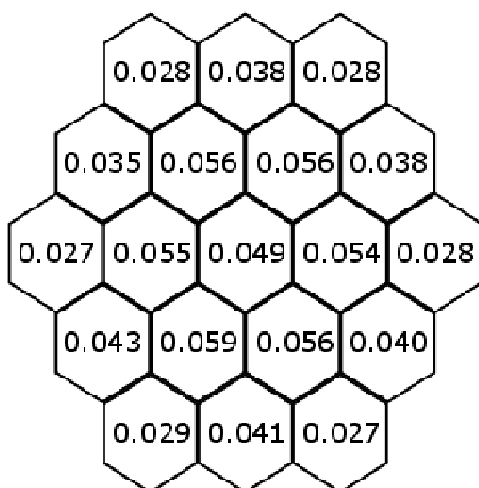


Fig. 5. Relative importance for smoothed and scaled pressure values associated with the most informative frame for the random forest classifier.

forest classifier are summarized in Table I. Note that as the number of classes is 6, random classification on average gives a rate of correct class prediction equal to 16.7%.

Standard evaluation of feature importance revealed that the most important feature was the largest scaled deviation (relative importance 0.216). Relative importance for smoothed and scaled pressure values associated with the most informative frame is shown in Fig. 5.

B. K -nearest neighbors classifier

For k -nearest neighbors classifier cross-validation showed that an optimal series for noise filtration in the most informative frame contains 8 frames, including 3 preceding the most informative one and 4 following it, with an exclusion of frames which do not satisfy conditions $1500 \leq S \leq 2900$; $0.1S_{inf} \leq S \leq 2.0S_{inf}$. Furthermore, cross-validation showed that the optimal metric is the Euclidian one, the optimal value of k is 1 (i.e., a simple model of one nearest neighbor), but that the optimal value of M is 10.

For these parameters the results of application of a k -nearest neighbors classifier are summarized in Table II.

Changing the value of k from 1 to 2 had a negligible impact on the classification results. However, further increase of k progressively reduced the accuracy, doubling the average number of classification errors in multiple cross-validation for $k=4$ and tripling for $k=10$.

Table I. Results for a random forest classifier. Rate of correct class prediction (%) is specified for the training set (mean value for testing part for multiple cross-validations) and for the validation set.

Sample class	Testing set (mean for 5-fold cross-validation)	Validation set
E-type	99.0%	87.5%
LF-type	98.2%	85.0%
LC-type	99.8%	70.0%
SF-type	93.0%	35.0%
SC-type	96.1%	65.0%
T-type	100%	70.0%
Total	97.7%	68.8%

Table II. Results for a k -nearest neighbors classifier. Rate of correct class prediction (%) is specified for the training set (mean value for testing part in multiple cross-validations) and for the validation set.

Sample class	Testing set (mean for 5-fold cross-validation)	Validation set
E-type	99.3%	97.5%
LF-type	100%	95.0%
LC-type	100%	30.0%
SF-type	97.9%	30.0%
SC-type	97.6%	90.0%
T-type	98.1%	95.0%
Total	98.8%	72.9%

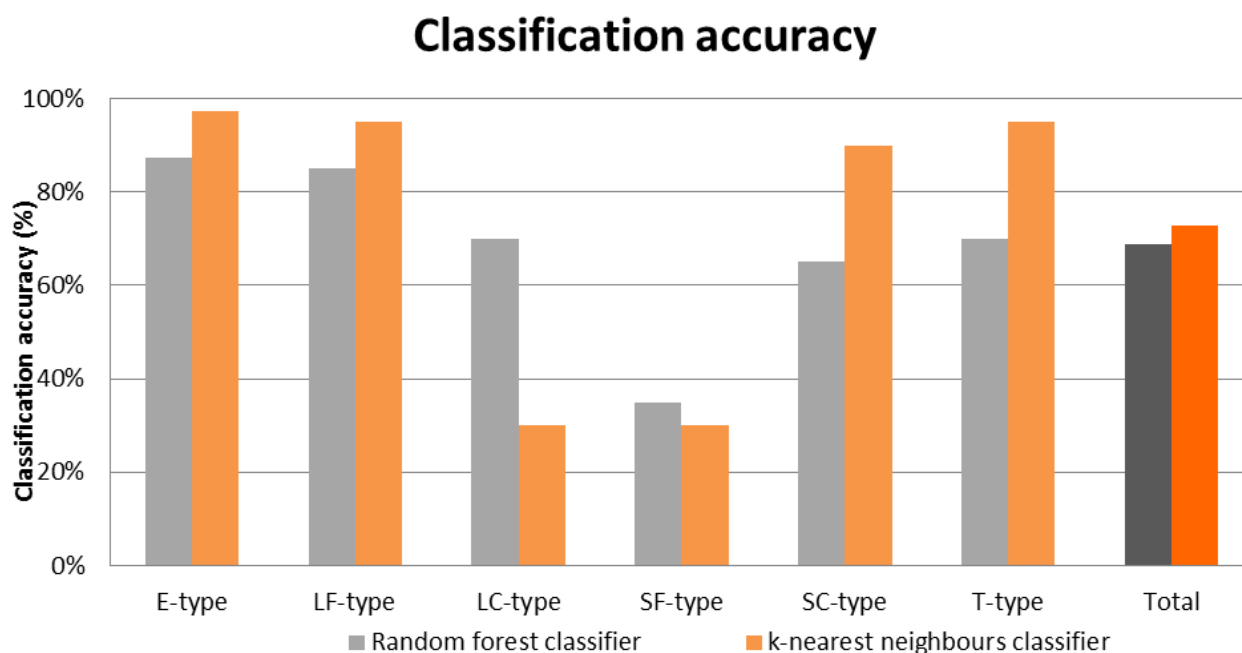


Fig. 6. Per-class and total classification accuracy provided by random forest classifier and nearest-neighbor classifier for the validation set .

IV. DISCUSSION

A. Evaluation of classification results

Presented results show that despite very limited resolution (both in terms of a number of tactile pixels and a number of discretization levels) tactile images registered by MTEC can be successfully classified even in case when classes are very similar and have only a slight difference either in embedment size or curvatures. It is worth noting that classification performed by volunteers based on conventional palpation by a finger had resulted in error rate comparable to the one observed for automated classification and the validation set.

High classification reliability was achieved by applying widely used machine learning methods – random forest classifier and k -nearest neighbors classifier – to a set of features specific to tactile images and additionally by applying an image cloning trick that is also specific to the studied image type.

The selected classification methods are essentially different. K -nearest neighbors approach in fact does not require training and it treats all features uniformly. On the contrary, random forest classifier requires non-trivial training and treats features ununiformly, as they are generally distributed ununiformly among decision trees and inside decision trees comprising a random forest. In spite of these differences the constructed random forest classifier and k -nearest neighbors classifier provided comparable classification accuracy, with a slightly higher result for k -nearest neighbors.

Interestingly, for random forests the rate of correct classification on the validation set was generally similar for

almost all classes, with an exception of SF-type samples. At the same time, for k -nearest neighbors classification the major difficulty was associated with discrimination of LC-type and SF-type samples, whereas other classes were recognized nearly perfectly (error rate equal to 10% for SC-type samples and not exceeding 5% for the other types). These results are illustrated in Fig. 6.

An essential role in achieving good classification reliability belonged to a proper selection of the feature set. The utilized feature set combined static data (pressure values in the most informative frame) with dynamic values (standard deviation of measurements for a sensor). Fig. 5 shows that among static features the most valuable information for the classification was provided by measurements performed by sensors located in the middle sensor ring.

Though only one dynamic feature was used in case of random forests, it essentially contributed to the classification reliability. Exclusion of dynamic features resulted in a reduction of correct class prediction rate for the validation set to the values 60.4% and 66.7% for random forest and k -nearest neighbors classifier, respectively.

The selected feature space did not only provide dimension reduction. It also provided robustness with respect to unavoidable differences in pressing parameters, e.g., pressing speed.

B. Directions for the future research

In our future research we plan to expand and deepen the results of the present study in several directions.

The first direction is adaptation and evaluation of other machine learning approaches using the constructed library of

instrumentally registered tactile images. The next method we are going to consider is the Support Vector Machine [16].

The second direction is further adaptation of k -nearest neighbors and other metric-based classification methods to tactile images. Our preliminary results show that the following ideas provide a substantial increase of classification quality. Classification can be applied to all tactile frames in an image (not only to one most informative frame) and the final identification of a class can be done using a voting scheme. This approach enables real-time image analysis, which is highly demanded by medical applications. In addition, classification can use a specially developed metric (or a generalized metric) instead of Euclidian distance. This metric should partially compensate the following drawbacks of Euclidian distance:

- tactile frames from the same image associated with different time moments are distant as larger pressing force increases all registered pressure values;
- rotations and shifts of an operating head of a MTEC mechanoreceptor essentially changes registered tactile frames leading to distant frames in case of multiple examinations of the same sample.

Currently we are testing the following generalized metric function which is based only on static data associated with two tactile frames

$$d(f_j, f_i) = \min_{\alpha, \rho} \|f_j - [\alpha \rho(f_i)]\|_p.$$

Here f_j and f_i are the compared frames (treated as points in a vector space which dimension coincides with the number of mechanoreceptor sensors), α is a non-negative number, ρ is a transformations of the vector space, $\|\cdot\|_p$ is the l_p norm ($p \geq 1$; for $p = 2$ it is the Euclidian norm), and $[\cdot]$ is a coordinate-wise cut

$$[x] = \begin{cases} x, & x \in [0, 255], \\ 0, & x < 0, \\ 255, & x > 255. \end{cases}$$

Minimum is taken over all nonnegative α and all transformations ρ from a predefined set. This set includes transforms associated not only with rotations of an operating head by angles multiple to 60° and with symmetric reflections, but also with shifts of an operating head (note that transforms associated with shifts use extrapolation).

Besides testing a new generalized metric specifically developed for analysis of tactile images, we also test generalizations of conventional k -nearest neighbors approach which take into account distributions of intra-class and inter-class distances.

Another direction of our future research focuses on application of machine learning methods to identification of heterogeneity in tactile images. The problem here can be formulated as a binary classification discriminating homogeneous and heterogeneous tactile samples. This problem is central for clinical applications of MTEC, where it is used mainly for the detection of lesion boundaries. The problem seems to be simple, but deviations of a contact angle from 90°

essentially complicate its solution [8], [9], [13]. A combination of relatively straightforward methods [9], [13] provides only a partial solution. Our preliminary results show that nearly perfect results can be achieved by using Support Vector Machine with the Radial basis function kernel.

Finally, along with applications of supervised machine learning method we plan to study the applications of unsupervised methods. Recently we proposed a novel clustering method [14] based on interval pattern concepts [17], [18] and showed that it outperforms conventional k -means clustering [19] in tactile images analysis. We expect to gain additional improvement by further optimization of the utilized feature space. We also plan to test other clustering techniques, including hierarchical clustering [20], spectral clustering [21] and density clustering [22], [23]. Our particular expectations are associated with the density clustering approach.

V. CONCLUSION

Automated analysis of instrumentally registered tactile images is a novel problem that is currently demanded by medical applications but definitely will soon be important for many other domains as well. Our results show that a combination of conventional machine learning methods with a specific feature set and specific tricks provides highly reliable results of automated analysis even in case of nontrivial tasks such as sample classification with very similar classes. These results are achieved in spite of very limited resolution of tactile images.

ACKNOWLEDGMENT

The authors thank Dr. Alexey V. Galatenko, Dr. Vladimir V. Galatenko, Dr. Vladimir M. Staroverov and Dr. Rozalia F. Solodova for valuable comments and discussions.

REFERENCES

- [1] V. Egorov and A. P. Sarvazyan, "Mechanical imaging of the breast," *IEEE Trans. Med. Imag.*, vol. 27, no. 9, pp. 1275–1287, Sep. 2008.
- [2] V. Egorov, H. van Raalte, and A. P. Sarvazyan, "Vaginal tactile imaging," *IEEE Trans. Biomed. Eng.*, vol. 57, no. 7, pp. 1736–1744, July 2010.
- [3] H. van Raalte and V. Egorov, "Tactile imaging markers to characterize female pelvic floor conditions," *Open J. Obstet. Gynecol.*, vol. 5, no. 9, pp. 505–515, Aug. 2015.
- [4] R. E. Weiss, V. Egorov, S. Ayrpetyan, N. Sarvazyan, and A. Sarvazyan, "Prostate mechanical imaging: a New method for prostate assessment," *Urology*, vol. 71, no. 3, pp. 425–429, Mar. 2008.
- [5] V. Barmin, V. Sadovnichy, M. Sokolov, O. Pikin, and A. Amiraliev, "An original device for intraoperative detection of small indeterminate nodules," *Eur. J. Cardiothorac. Surg.*, vol. 46, no. 6, pp. 1027–1031, Dec. 2014.
- [6] R. F. Solodova et al., "Instrumental tactile diagnostics in robot-assisted surgery," *Med. Devices (Auckl.)*, vol. 9, pp. 377–382, Oct. 2016.
- [7] R. Solodova, V. Galatenko, E. Nakashidze, V. Staroverov, and M. Sokolov, "A novel method for intraoperative tactile examination in colorectal surgery," presented at the 29th Conf. of the International Society for Medical Innovation and Technology, Torino, November 9–10, 2017, Paper O10.
- [8] R. F. Solodova et al., "Instrumental mechanoreceptor palpation in gastrointestinal surgery," *Minim Invasive Surg.*, to be published.

- [9] R. Solodova et al., "Automated detection of heterogeneity in medical tactile images," *Stud. Health. Technol. Inform.*, vol. 220, pp. 383–389, 2016.
- [10] L. Breiman, "Random forests," *Mach. Learn.*, vol. 45, no. 1, pp. 5–32, Oct. 2001.
- [11] T. Cover and P. Hart, "Nearest neighbor pattern classification," *IEEE Trans. Inf. Theory*, vol. 13, no. 1, pp. 21–27, Jan. 1967.
- [12] Z. Zhang, "Introduction to machine learning: k-nearest neighbors," *Ann. Transl. Med.*, vol. 4, no. 11, article 218, Jun. 2016.
- [13] V. M. Staroverov et al., "Automated real-time correction of intraoperative medical tactile images: sensitivity adjustment and suppression of contact angle artifact," *Appl. math. sci.*, vol. 10, no. 57, pp. 2831–2842, Sept. 2016.
- [14] S. A. Nersisyan, V. V. Pankratieva, V. M. Staroverov, and V. E. Podolskii, "A greedy clustering algorithm based on interval pattern concepts and the problem of optimal box positioning," *J. Appl. Math.*, Article ID 4323590, Sept. 2017.
- [15] F. Pedregosa et al., "Scikit-learn: machine learning in Python," *J. Mach. Learn. Res.*, vol. 12, pp. 2825–2830, Oct. 2011.
- [16] C. Cortes and V. Vapnik, "Support-vector networks," *Mach. Learn.*, vol. 20, no. 3, pp. 273–297, Sept. 1995.
- [17] B. Ganter and R. Wille, *Formal concept analysis: mathematical foundations*. Berlin, Germany: Springer, 1999.
- [18] B. Ganter and S. O. Kuznetsov, "Pattern structures and their projections," in *Conceptual Structures: Broadening the Base*, vol. 2120 of *Lecture Notes in Computer Science*, Springer Berlin Heidelberg, Berlin, 2001, pp. 129–142.
- [19] D. Steinley, "K-means clustering: a half-century synthesis," *Br. J. Math. Stat. Psychol.*, vol. 59, no 1, pp. 1–34, May 2006.
- [20] F. Murtagh and P. Contreras, "Algorithms for hierarchical clustering: an overview," *WIREs Data Mining Knowl. Discov.*, vol. 2, no.1, pp. 86–97, Jan./Feb. 2012.
- [21] U. von Luxburg, "A Tutorial on Spectral Clustering," Max Planck Institute for Biological Cybernetics, Techn. Rep. No. TR-149, Mar. 2007.
- [22] M. Ester, H.-P. Kriegel, J. Sander, and X. Xu, "A density-based algorithm for discovering clusters in large spatial databases with noise", in *Proc. 2nd Int. Conf. on Knowledge Discovery and Data Mining (KDD-96)*, Portland, OR, 1996, pp. 226–231.
- [23] C. Jinyin, H. Huihao, C. Jungan, Yu Shanqing, and Shi Zhaoxia, "Fast Density Clustering Algorithm for Numerical Data and Categorical Data," *Math. Probl. Eng.*, vol. 2017, Article ID 6393652, Mar. 2017.